JOINT INSTITUTE FOR NUCLEAR RESEARCH
Frank Laboratory of Neutron Physics

Final Report on the Summer Student Program

A whole new line of thinking into vitamin C

Supervisor:
Prof. Dr. Sc. A. Filarowski

Student:
M. Sc. Kinga Jóźwiak, Poland
Chemistry Department
University of Wroclaw

Participation period:
August 01 – August 31

Dubna, 2021

Contents

1. Abstract

The research project *"A whole new line of thinking into vitamin C"* was being prepared in Frank Laboratory of Neutron Physics (FLNP) in Joint Institute for Nuclear Research (JINR) in Dubna, Russia. Although the molecule of our research is widely known in the world of scientists and medics, many properties and applications have not yet been discovered.
Due to the different biological activity of individual ascorbic acid isomers, two diastereoisomers were tested in the project: L-ascorbic acid and D-isoascorbic acid. Moreover, studies of their deuterated derivatives have also been performed.

The main purpose of the project was to correlate non-covalent interactions (hydrogen bond) with spectroscopic parameters. To achieve this goal many research methods were used in the project. The experimental techniques include: IINS (Inelastic Incoherent Neutron Scattering) spectroscopy, IR spectroscopy (two ranges: MIR – Mid-Infrared and FIR – Far-Infrared) and Raman spectroscopy. Additionally, the quantum mechanical methods were used to analyze the studied molecule: DFT (Density Functional Theory), CPMD (Car-Parrinello Molecular Dynamics) and PED (Potential Energy Distribution). The combination of all methods: experimental and computational allowed for a complete analysis and interpretation of the studied molecule.

The final report was divided into two parts: theoretical part and the result part. The first part describes the properties of vitamin C, its chemical structure and potential use as a drug in the fight against the COVID-19 virus. Moreover, neutron scattering, IINS spectroscopy and measuring equipment - NERA spectrometer have been described in details. This section also includes a description of the isotope effect (especially H/D isotope effect). The second part of the report includes the spectra obtained with the IINS, IR, Raman methods and their detailed interpretation thanks to the use of computational methods (PED, CPMD, DFT). Moreover, curves of potential energy for proton transfer in hydrogen bridges in ascorbic acid isomers (L-ascorbic acid and D-isoascorbic acid) are also presented and interpreted.

2. Introduction

Introducing the topic of a scientific project, I would like to quote the words *"Vitamins are organic molecules that are required in microgram to milligram amounts for health, growth, and reproduction".*[1] These organic compounds are marked by diverse chemical and physical properties. Vitamin C, which is the object of research, water-soluble vitamin like folate, pantothenic acid, biotin. Adequate supplementation of ascorbic acid has a positive, preventive impact on health. Especially in disorders such as common cold, some cancers and cardiovascular diseases *(Fig. 1).*[2]

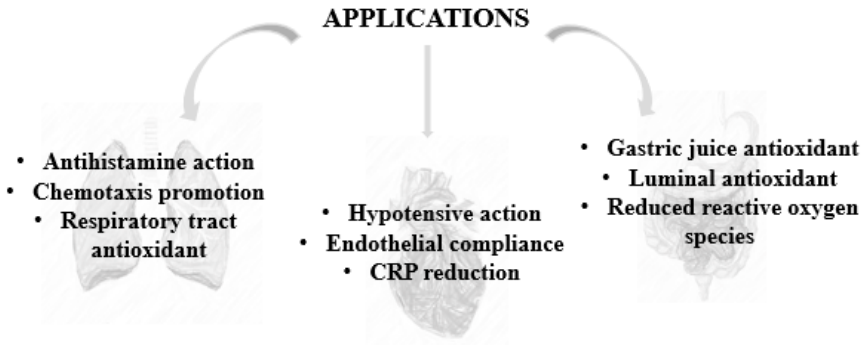

Figure 1. Positive impact appropriate vitamin C supplementation on various diseases. states.[2]

Moreover, in the human body, ascorbic acid is also attended in countless organic syntheses, as a cofactor. Norepinephrine (NA) which belongs to the group of catecholamines is the principal transmitter of sympathetic postganglionic fibres and certain tracts of the central nervous system.[3] Biosynthesis of noradrenaline is feasible by essential cofactor, which is vitamin C. The main function of ascorbic acid is to hold Cu in a reduced form in complex with dopamine-b-hydroxylase which is necessary for the proper reaction.[4] Serotonin (5-hydroxytryptamien, 5-HT), neurotransmitter which is related to emotional aspects of human behavior like anxiety or depression, is synthesized by hydroxylation and decarboxylation of tryptophan.[5] Ascorbic acid is required in order to obtain serotonin in the first step of hydroxylation catalyzed by tryptophan hydroxylase. Other but also important syntheses for the body in which ascorbic acid is essential are for example carnitine which is synthesized from lysine and methionine by some hydroxylases. Lack of right amount of vitamin C lead to decrease the rate of carnitine biosynthesis and the productivity of renal reabsorption of carnitine.[6]

Vitamin C is characterized as an organic compound with a versatile and necessary action that brings positive effects on human health. Despite so many scientific works about this molecule, the properties of ascorbic acid are still being researched and rediscovered.

3. Characteristics of the studied molecule

3.1. Molecular structure

Vitamin C (ascorbic acid), lactone of 2-keto-l-gulonic acid is a derivative of saccharides. It is characterized by strong reducing properties and acidic character thanks to the presence in the structure of the enediol group. What is more, the various tautomeric forms of ascorbic acid are capable of reacting. Ascorbic acid isomers, despite the same elemental composition, differ in their properties, hence the study during the project as many as two of the four isomeric forms *(Fig. 2).*

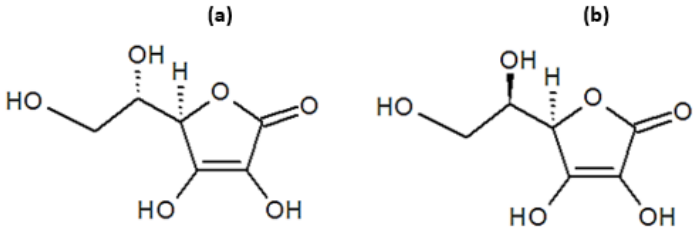

Figure 2. Chemical structures of studied (a) L-ascorbic and (b) D-isoascorbic acids.

3.2. Medicament to defeat the coronavirus disease

Vitamin C properties such as antioxidant activity which protect molecules from oxidative damage and its main role in the proper functioning and regulation of the immune system made it possible to use vitamin as a drug in the fight against COVID-19. Coronavirus (RNA virus, zoonotic virus) in the family *Coronaviridae* of the order *Nidovirales* attacks the human respiratory system.[7] The interest in vitamin C as a drug used to treat the virus is also supported by the many positive effects of vitamin enabling the proper functioning of the human lung.

Nowadays, there are countless oral medications containing vitamin C. Despite this, the amount of the preparation in the treatment of sick people is insufficient. However, administration of a high dose of the preparation requires intravenous administration which is necessary in sick patients. Numerous studies show that within 24 hours of critical illness, acute injury, multiple organ failure or sepsi the level of vitamin C drops significantly.[8]

The research results published in *The Pediatric Infectious Disease Journal* showed that the use of vitamin C supplementation significantly reduces the incidence of pneumonia, confirming the effectiveness of the drug.[9] A number of studies have also been carried out to check the adverse effects of vitamin C in therapy. For example, Nathens's publication[10] clearly

presents the results of studies in which it was administered to patients 1 gram of ascorbic acid every 8 hours for 28 days if not for adverse effects occurred.[11]

All of the above information indicates that vitamin C therapy is likely to be effective. Vitamin C dosing causes reduces the impact oxidative stress and cytokine. A number of studies have been carried out to show that the administration of vitamin C infusions of 200 mg/kg body weight in 4 doses reduces clinical symptoms in infected individuals and decreases in mortality of COVID-19 patients. What is more, patients who received dose 6 g daily orally significantly reduces the risk of infection with the virus. Additionally, dose of 10 g and 20 g per day, given over a period of 8–10 h administered in China, improved the oxygenation index.[12]

4. Neutron spectroscopy

4.1. Neutron

Neutrons, elementary particles represent one of the two nucleons in the nucleus. The mass of the neutron amounts 1.674928 (1) $\cdot 10^{-27}$ kg. Compared to the other constituents of the atomic nucleus, it is a mass very similar to a proton and slightly more different from an electron. The internal structure of a neutron is described by quarks: two "down" quarks and one "up" quark. The magnetic moment is closely related to the spin of the neutron and takes a value $\mu = -9.6491783(18) \cdot 10^{-27}$ JT^{-1}. The neutron is an unstable particle decaying to a proton, electron and antineutrino with an average lifetime of $\tau = 885.9\ (8)$ s.[13,14]

The neutron is a powerful tool for the study of condensed matter. It has a significant advantage over other types of radiation in the study of microscopic structure and dynamics. Due to the fact that they have no charge and their electric dipole moment is negligible, neutrons can penetrate through thick layers of different types of materials. The movement of neutrons is not disturbed by charged particles included in atoms, and the interaction with atoms is mainly carried out by nuclear forces.[15,16]

4.2. Neutron scattering

Scattering is a *"physical process in which some forms of radiation, such as light, sound and moving particles, are forced to deviate from a straight trajectory by one or more localised nonuniformity in the medium through which they pass"*.[13] The number of scattered neutrons (spectral intensity) is characterized by the law of scattering:

$$S\,(Q,\omega_v)_j^n \propto \sigma_j \frac{(Q \cdot U_{v_j})^{2n}}{n!} \exp\left(-\left(Q \cdot \sum_v U_{v_j}\right)^2\right)$$

where Q – momentum transfer, ω_v - vibrational frequency, j – given atom, v - vibrational mode, U_v - amplitude of vibration, σ_j - the cross-section of atom j, n - the order of the final state of the mode excited by the neutron.

Neutron scattering are based on influence neutron beam on the sample. The described neutron beam is characterized by: energy E_0, wave vector $\vec{k}_0$, wavelength λ_0. As a result of the interaction of the neutron beam with the system, marked as $V(\vec{r}, t)$ the beam is described by E_1 and $\vec{k}_1$. Equation presents the energy of neutrons:

$$E = \hbar\omega = \frac{\hbar^2\left|\vec{k}\right|^2}{2m_n}$$

where $\vec{k}$ – wavevector, m_n – mass of neutron, $\hbar$ - the Plank constant.[17]

Inelastic neutron scattering can be represented by *scattering triangle*, where 2θ presents neutron deflection angle and Q ($\vec{Q} = \vec{k}_0 - \vec{k}_1$), which is *scattering vector (Fig. 3).*

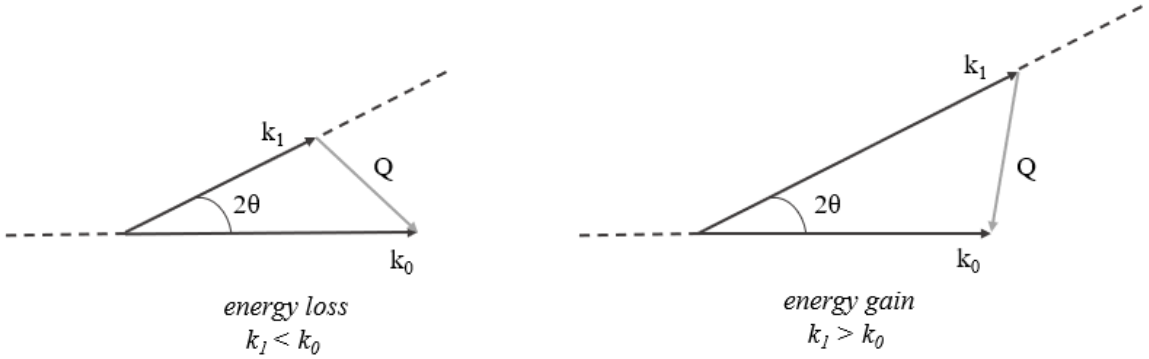

Figure 3. Loss ($k_1<k_0$) and gain ($k_1>k_0$) of neutron energy due to interaction with the sample – inelastic neutron scattering.[17-19]

For inelastic interactions (where $(\hbar\omega \neq 0)$) the scattering vector (Q) is dependent on angle θ. This principle is shown in the equation below:[17-19]

$$\frac{Q^2}{k_0^2} = 2 - \frac{\omega}{\omega_0} - 2cos(2\theta)\sqrt{1 - \frac{\omega}{\omega_0}}$$

Neutron scattering is also dependent on the type of scattering medium. The predominant type of scattering is incoherent scattering, which depends on the movements of individual atoms of a given molecule. The parameter that describes the area of a given nucleus in which the neutron beam has been scattered is called the cross-section. The cross section is marked with the symbol σ and the units are barns (1 barn = 10^{-24} cm^2):
$\sigma = 4\pi b^2$, where b – thermal neutron cross-sections.[19-20]

4.3. IINS method

The IINS method was used during the research project. IINS stands for Inelastic Incoherent Neutron Scattering and uses a neutron beam that interacts "inelastic" (change of direction and size of the neutron wave vector) and "incoherently" (independent interaction with each nucleus in the sample without interfering) with the atomic nucleus. Presented type of vibrational spectroscopy allows to obtain information on all the waves allowed by the symmetry of the crystal and the size of the crystal cell. Compared to IR or Raman, spectroscopy research using this method is not limited by selection rules. The IINS method is called the hydrogen sensitive method. This is due to the fact that hydrogen is much larger quantity σ^{incoh} compared to other nuclei *(Tab. 1).* Hence, the spectrum shows mainly signals from the hydrogen transitions. It is an important feature of the method that enables the research of e.g. isotope effect or hydrogen bonding.[20-21]

Table 1. Comparison of nuclei, their spins and numerical value of σ^{incoh} [b].[20-21]

Nucleus	*Spin*	σ^{incoh} *[b]*
N	1	0.3
D	1	2.0
H	½	79.7
O	0	0.04
C	0	0.01

4.4. Inverted geometry time-of-flight (TOF) spectrometers

The TOF (Time-of-flight) is an ever-evolving technique for measuring the time neutrons travel from the source to the detector. This distance is a known quantity. Due to the interaction of the neutron with the sample, its energy changes, which is proportional to the change in time. There are two types of TOF spectrometers: direct and indirect (e.g. NERA, JINR, Dubna, Russia) geometry spectrometers *(Fig. 4).*[22,23]

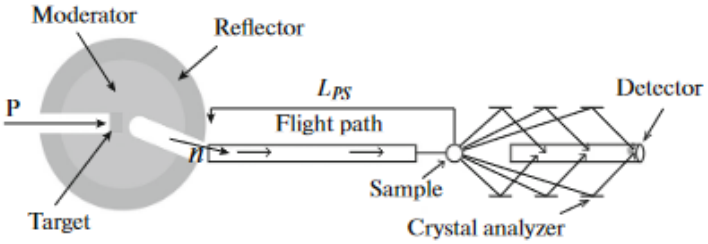

Figure 4. Schematic of the indirect-geometry neutron spectrometer.[18]

Inverted geometry time-of-flight (TOF) spectrometers make up a diverse range of spectrometers located all over the world for example in Europe, United Stated, Japan or Russia. The specimen is lighted by a white chink of light. Their operation is explained by determination of the incoming neutron energy or velocity. This is done by determining the time elapsed between the source pulse and the detection. The analysis and interpretation of the final energy of the neutrons is possible thanks to the operation of crystal analyzers located in front of the detectors.[24,25]

4.5. NERA

NERA is one of 18 measuring instruments, creating a multi-functional, pulsed IBR-2 reactor system. The NERA spectrometer belongs to the group of inverted geometry time-of-flight (TOF) spectrometers. It works by registering scattered neutrons of specific energy. It enables the measurement of e.g. phase transitions, polymorphism or molecular dynamics.[26,27]

The source of the neutrons is the IBR-2 reactor, the main part of which is an irregular hexagon. The reactor produces fast electrons. Cooling takes place thanks to the presence of sodium and a system consisting of many circuits and loops. The device also has the ability to periodically modulate the reactivity by rotating the main and auxiliary reflectors. The pelletized moderator based on aromatic hydrocarbons makes possible e.g. cold neutron yield, low radiolytic hydrogen release, security. Neutrons with a certain energy are transported from moderators of radial horizontal beamlines 7-11 and tangential beamlines 1–9 to the sample position at L_1 = 109.05 m. Slowing down the neutrons, isolating neutrons with a specific energy value and the incident of a collimated beam on the sample enable: beam shutter, fast neutron background chopper, common vacuum splitter of three neutron beams by Ni-mirror neutron guides, l-chopper of beamline 7b, vacuum Ni-mirror guide tube of neutron beamline 7b, vacuum sections of beamline 7b, monitor and diaphragms of incident beam 7b. The parameters characterizing the NERA spectrometer are presented in *Table 2.*[27-30]

Table 2. Parameters of the NERA spectrometer.[27-30]

Neutron guide	*Ni, mirror, vacuum*
Guide aperture	50·160 mm^2
Thermal neutron flux and sample position	$4.6 \cdot 10^6$ $n/cm^2/s$
Wavelength range	0.4-7.0 Å
Scattering angles range	10° - 170°
Energy transfer range (INS)	ω=0-130 meV

Moderator – sample distance	109.5 m
Sample – detector distance	0.815 m (INS with Be-filter) 1.015 m (INS with single crystal) 1.415 m (neutron diffraction)
Resolution *Inelastic scattering*	Δω/ω=2-4%
Neutron diffraction	Δd/d=0,4% for λ>1 Å

An example of a device belonging to the same type of spectrometers (inverted geometry time-of-flight (TOF)) is TOSCA instrument, located in TS-1 at ISIS Neutron and Muon source, Chilton, UK *(Fig. 5).* The measurements performed on this type of spectrometer are performed within the range 0-500 meV. The operation of the spectrometer is based on the scattering of a neutron beam incident on the sample, which is then reflected by a pyrolytic graphite analyzer. Then, the neutrons are transported to the beryllium filter. The specified wavelengths are sent to the 3He tubes bank. Spectrometer is equipped with closed cycle refrigerator enables measurements in a wide temperature range. Spectrometer measurements are made for different chemical compounds like organic, biological samples or hydrogen bonded systems.[31,32]

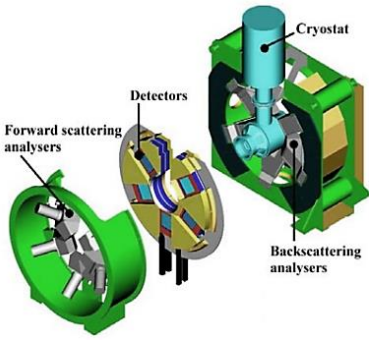

Figure 5. Schematic of TOSCA.[32]

To compare the resolution of both spectrometers: NERA and TOSCA, the inelastic neutron scattering spectra were measured. Triphenylmethane (TMP) was the subject of research. TMP is hydrocarbon with the formula $(C_6H_5)_3CH$. The temperature range was 10-22 K. Research has shown that both in the low frequency range (ring vibrations) and higher frequencies (tensile vibrations), the TOSCA spectrometer has a higher resolution *(Fig. 6)*.[32]

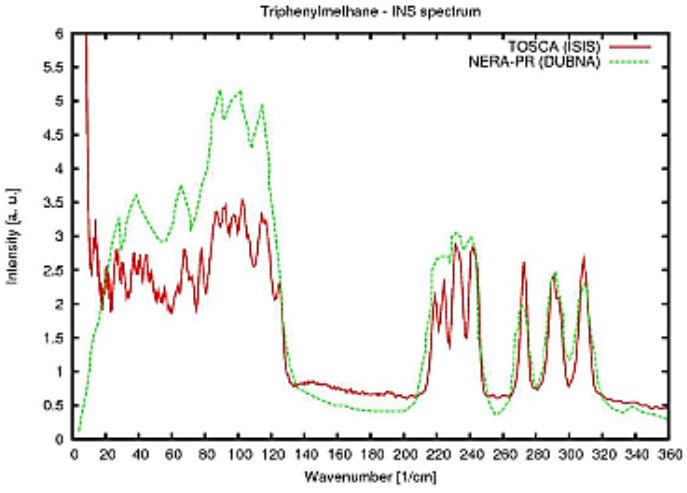

Figure 6. INS spectra of TMP measured at TOSCA and NERA-PR spectrometer in the energy transfer region between 0 and 350 cm^{-1}.[32]

5. H/D isotope effect

In 1766 Henry Cavedish[33] (English chemist and physics) for the first time proved that hydrogen (^{1}H) is a separate chemical element. English scientist performed two chemical reactions, discovering the first properties of hydrogen: 1) dissolving metals in dilute acids and isolated hydrogen; 2) the resulting gas, when mixed with air, explodes violently in the presence of a heat source (flame). Not long after that, a French chemist Antoine Lavoisier[34] in named the gas hydrogen from the Greek words, *"hydro"* and *"genes".* In the following years, other but extremely significant properties and possibilities of using hydrogen were discovered e.g. electrolysis, renewable hydrogen, rocket propulsion, fuel for fuel cells.[35,36]

The first element of the periodic table (^{1}H) despite the presence of only one electron and one proton in its structure, has as many as seven isotopes. These are three naturally occurring isotopes *(Fig. 7):* hydrogen (^{1}H), deuterium (^{2}H) and tritium (^{3}H), and four artificially produced (^{4}H, ^{5}H, ^{6}H, ^{7}H).[35,36]

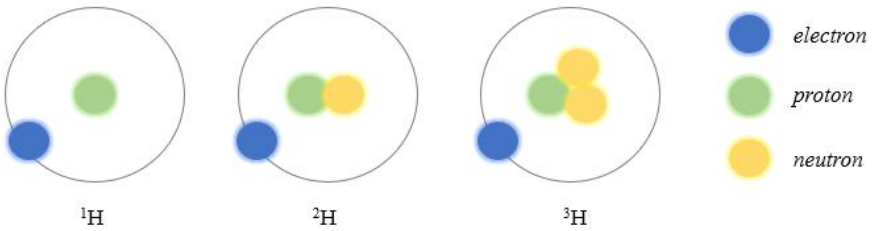

Figure 7. Atomic structure of hydrogen (^{1}H), deuterium (^{2}H) and tritium (^{3}H).

The term isotope is defined as *one of two or more species of atoms of a chemical element with the same atomic number and position in the periodic table and nearly identical chemical behavior but with different atomic masses and physical properties*.[37] In chemistry, the most popular isotopes that are used for research are not radioactive, stable hydrogen and deuterium. To study chemical molecules that contain hydrogen bonds in their structure, it is important to study the H/D isotope effect. Isotope effect (IE) is *difference in some molecular or atomic property consequent to a change in mass or mass distribution caused by isotopic substitution*.[38] There are few rules of this effect. Firstly, it depends on the isotope masses and the forces that bind the atom at the isotopic substitution site. Secondly, there are constant changes in force at the side of isotopic substitution. Thirdly, the additivity of isotope effects is so important.

IEs $\left(\frac{K_{light}}{K_{heavy}}\right)$ values vary depending on the isotopes that are substituted. For example, the H/D substitution is characterized by a higher $\frac{K_{1_H}}{K_{2_H}}$ ratio compared to $\frac{K_{14_N}}{K_{15_N}}$, so when the difference in mass of both isotopes is smaller, IEs also decreases *(Equilibrium 1,2, below)*.[38,39]

Equilibrium 1

$H_2 + 2DI \rightleftharpoons D_2 + 2HI$ $\qquad \frac{K_{1_H}}{K_{2_H}} = 1.210$

Equilibrium 2

$^{15}NH_3 + {}^{14}NH_4^+ \rightleftharpoons {}^{14}NH_3 + {}^{15}NH_4^+$ $\qquad \frac{K_{14_N}}{K_{15_N}} = 1.034$

When studying the H/D isotope effect, it is extremely important to know the dynamics of the hydrogen and deuterium atom and the resulting anharmonics. The hydrogen (^{1}H) and deuterium (^{2}H) bonding are characterized by potential energy curves. The zero point energy is different for both isotopes while for hydrogen vibrations the zero point energy level is higher. What is more, the amplitude of proton vibrations significantly exceeds the amplitude of deuterium vibrations which affects the stability of the formed hydrogen bridges.[39,40]

Research of the H/D isotope effect are undertaken by many researchers from various fields of physics and chemistry. There are studies conducted from high temperature perovskite proton conductors[41], positively and negatively charged water complexes[42], metal oxides[43] to charged water clusters[44] and others. Despite this, the study of IE is not limited to the areas presented, and their analysis and interpretation of results provide new possibilities and applications in many areas, i. e. medical, agricultural, polymer, material, pharmacological science; chemical physics; molecular and structural biology; biochemistry; biophysics; organic and inorganic chemistry *(Fig. 8).*

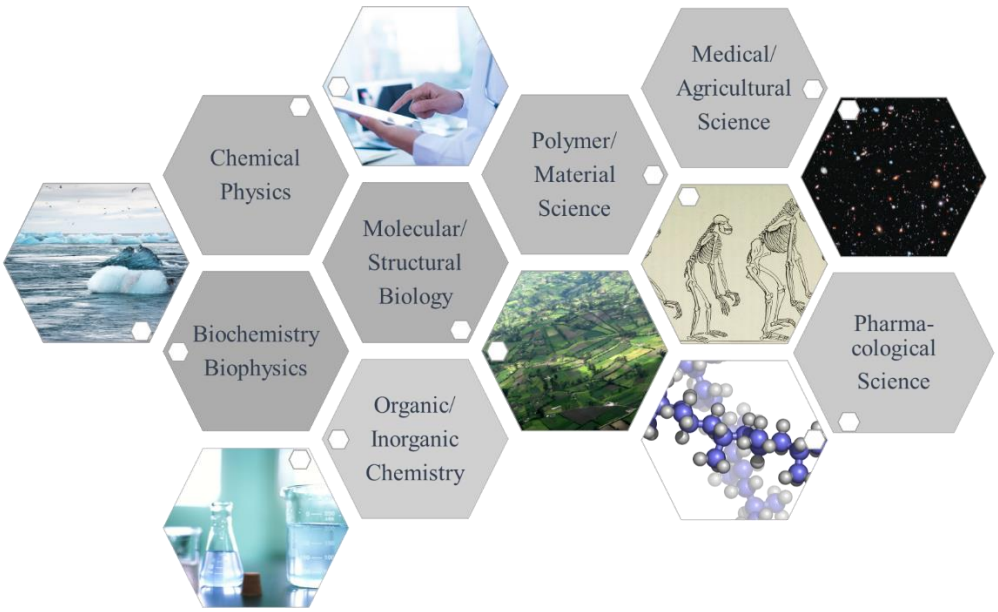

Figure 8. Diagram showing the scientific fields in which the isotope effect can be applied.

6. Description of deuteration and research methods

6.1. Deuteration

Deuteration was performed by dissolving the appropriate amount of L-ascorbic and D-isoascorbic acid in deuterated water D_2O (50 ml). The resulting solution was heated to a temperature around of 100 ^oC. Then the solvent was removed by evaporation under reduced pressure. The procedure for both isomers of ascorbic acid was repeated three times.

Deuteration was carried out before the practices at the Faculty of Chemistry of the University of Wrocław (Wrocław, Poland).

6.2. Experimental techniques

1. **IR spectroscopy**

The measurements were carried out in two spectral ranges: Far-Infrared (FIR) and Mid-Infrared (MIR) with Fourier transform. IR spectra measurements were made using a Bruker Vertex 70v spectrometer. The spectra were measured with a resolution of 4 cm^{-1}. The number of scans was 64 for each spectrum, respectively. Apiezon N Grease vacuum grease was used for FT-FIR measurements (range 600-50 cm^{-1}). The samples prepared for the measurement were placed on polyethylene (PE) plates. The KBr pellet technique was used to measure the FT-MIR spectra with the Fourier transform.

2. **Raman spectroscopy**

Raman spectra were obtained with a FT-Nicolet Magma 860 spectrophotometer. The radiation source was an In:Ga:Ar laser beam at 1064 nm. The spectra were measured in the range from 200 to 3800 cm^{-1}. The resolution was 4 cm^{-1} and the number of scans was 512.

3. **IINS spectroscopy**

IINS spectra were measured in an IBR-2 high flux pulse reactor using a NERA spectrometer at the Joint Institute for Nuclear Research (JINR) in Dubna, Russia. IINS spectra were measured at 5K. The spectral range was from 5 to 1700 cm^{-1} and resolution was 3%. The spectra were appropriately converted to the scattering functions S (Q, ω).

During the practice, thanks to the experimental data, IR, Raman and IINS spectra were processed. The IR and Raman spectra were measured on the equipment at the Faculty of Chemistry, University of Wrocław. IINS spectra were measured at the Joint Institute for Nuclear Research in Dubna, Russia during the operation of the IBR-2 reactor.

6.3. Quantum mechanical methods

1. DFT and PED calculations

The calculations were made using the Gaussian 16[45] software suite: PuTTY 0.60, Xming 6.9.0.31, WinSCP 4.1.9. For quantum mechanical calculations, the Density Functional Theory (DFT), B3LYP functional and 6-311+G (d, p) based on Pople's notation were used. The calculations were made in the gas phase for the basic state. On the basis of the structural formulas of ascorbic acid isomers, the molecular structures of the studied systems were constructed using the Molden program. The hydrogen mobility has been studied and potential energy profiles for proton transfer in intramolecular (monomers) and intermolecular (dimers) hydrogen bonds in the gas phase were calculated. The distance between the hydrogen atom and the oxygen atom was changed by elongating the O-H bond. During this operation other structural parameters were optimized for each step. The O-H bond length increment of 0.1 was used. The potential energy distribution (PED) of the normal modes was calculated in Gar2ped[46] program.

DFT calculations were made, analyzed and interpreted during practice and PED were made in collaboration with Dr. Sc. J. J. Panek from Faculty of Chemistry, University of Wrocław (Wrocław, Poland).

2. CPMD method

CPMD (Car-Parrinello molecular dynamics) was calculated in the gas and crystalline phases. The program necessary to perform the calculations was CPMD program Version 3.17.1. For the calculations in the gas phase, the structures obtained in the DFT calculations were used and in the solid phase – the X-ray data measurements. For calculations *in vacuo* models were stowed in cubic cells. For ascorbic acid monomers and dimers, these were cubic cells with dimensions a = 12 Å (for L-ascorbic acid monomer), a = 12.5 Å (for D-isoascorbic acid monomer), a = 19 Å (for L-ascorbic acid dimer) and a = 22 Å (for D-isoascorbic acid dimer). In contrast, the primitive cell sizes for phase calculations were different for the two isomers: a) for L-ascorbic acid: $\alpha = 90°$, $\beta = 99.355°$, $\gamma = 90°$, Z = 4, a = 6.4213 Å, b = 6.3622 Å, c = 17.1606 Å; b) D-isoascorbic acid: $\alpha = 90°$, $\beta = 99.50°$, $\gamma = 90°$, Z = 2, a = 5.165 Å, b = 14.504 Å, c = 4.724 Å. In the calculation of the crystalline phase applied periodic boundary conditions, real-space electrostatic summations for the eight nearest neighbors in each direction. Programs VMD 1.9.3[47], Mercury[48] and Gnuplot[49] were used to illustrate the final results.

CPMD calculations were made and processed thanks to cooperation with Dr. Sc. A. Jezierska, Dr. Sc. J. J. Panek from Faculty of Chemistry, University of Wrocław (Wrocław, Poland).

7. Experimental and computational data

Based on the IR spectra and Raman spectra, conclusions can be drawn about assigning bands to the appropriate vibrations of the fragments of ascorbic acid molecules (L and D-iso isomers). Within the measured spectral range, it is possible to assign bands to the stretching vibrations of the hydroxyl groups (ν_{OH}) of both isomers. The spectra of L-ascorbic acid show 6 ν_{OH} bands (2777, 3032, 3219, 3317, 3411, 3526 cm^{-1}). Interestingly, in the spectra of D-isoascorbic acid, there are only 4 bands assigned to this type of vibration (2745, 3016, 3334, 3482 cm^{-1}) *(Fig.10).* The deuteration process and measurement of the IR and Raman spectra of deuterated derivatives allowed to confirm the appropriate assignment of bands to the molecule vibrations. It is visible in the spectrum by shifting these bands after deuteration towards lower wavenumbers and ISR = 1.22 – 1.35 (OH→OD, marked on IR spectra *(Fig. 10)*). Due to the correlation of the experimental data with the CPMD calculation method, it was possible to accurately assign the bands to the stretching vibrations of the hydroxyl groups. The assignment of the bands applies to the hydroxyl groups located at the carbons marked with numbers 2, 3, 5, 6 *(Fig. 9).* The band located in the IR spectrum at 2777 cm^{-1} is assigned to the ν_{OH} vibrations marked in the ***3AA*** *(Fig. 9, structure 3AA)* while the band located at 3032 cm^{-1} was assigned to the vibration of the hydroxyl groups shown in the ***2AA*** structure *(Fig. 9, structure 2AA).* The series of bands located at higher fall numbers (3219, 3317, 3411, 3526 cm^{-1}) have been assigned to the ν_{OH} vibrations shown in the structures ***5AA***, ***6AA*** *(Fig. 9, structure 5AA, 6AA).*

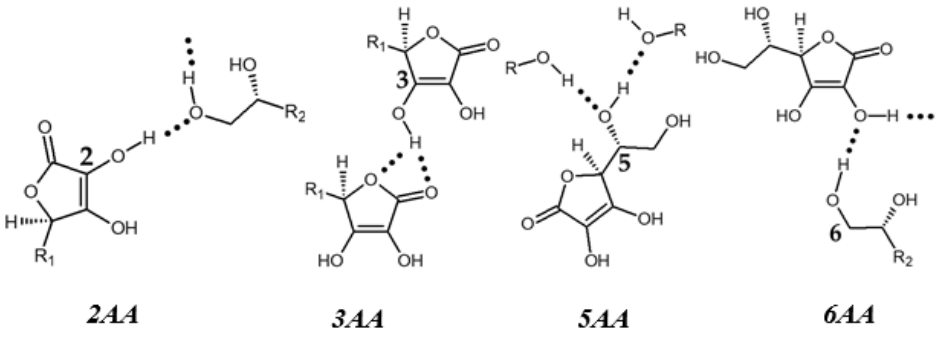

Figure 9. Schemes of ascorbic acid structures with marked hydrogen bonds and R (ascorbic acid), R1 (-CH(OH)CH_2OH), R2 (γ-lactone ring).

The hydrogen bonding for ***2AA*** is considered to be the strongest due to the greatest shift towards lower wavenumbers, which is equivalent to the shortest distance between oxygen and hydrogen

atoms. The more the described band is in the range of higher wavelengths, the distance between the donor and acceptor increases, so the strength of the hydrogen bonds formed decreases.

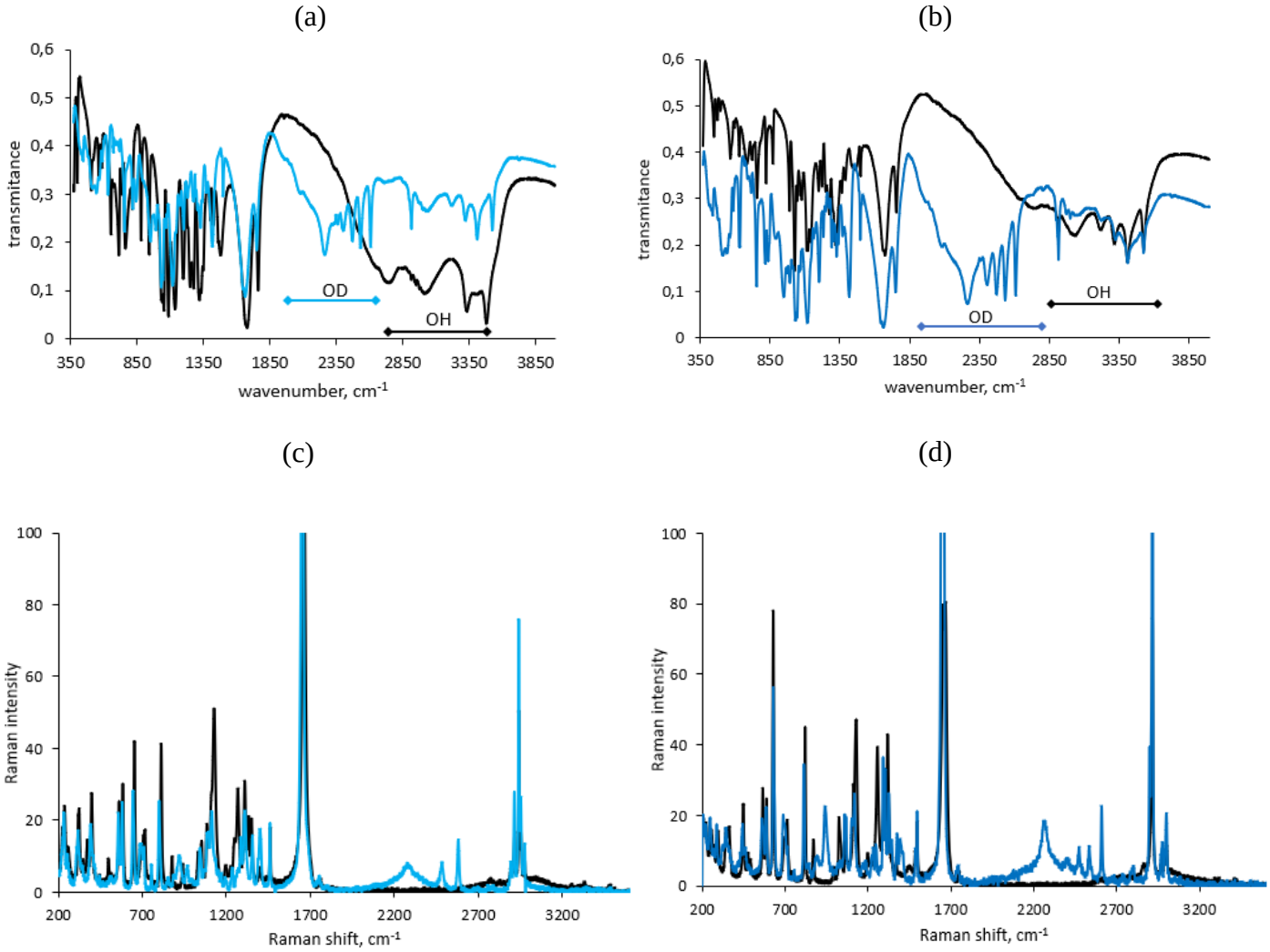

Figure 10. Normalized FT-MIR in region 350 - 3900 cm $^{-1}$(a-b) and Raman in 200 – 3600 cm^{-1} region (c-d) spectra of (a, c) D-iso- and (b, d) L-ascorbic acids (black spectra) and its deuterated derivatives (blue spectra. The band shift after deuteration for both isomers is shown in the MIR spectra.

In order to present the validity of the application of the IINS method to the study of ascorbic acid isomers, the spectra obtained by the IINS method were compared with the IR and Raman spectra. This method serves an extremely important role in the study of hydrogen bonding systems because it is possible to clearly observe the decrease in the intensity of OH bands after deuteration. This is due to the significant difference in the cross sections for hydrogen and deuterium. Thanks to this, it is possible to unambiguously assign bands to the vibrations of the hydrogen bridge of the system.

In the range of 1000-1500 cm^{-1} for L-ascorbic acid it is possible to observe eight bands whereas in the same region for the D isomer, only four bands are observed *(Fig. 11)*. These are bands that come from in-plane deformational vibrations (δ_{OH}). The certainty of assigning bands to this type of vibration is explained by the isotope effect. The isotope effect was also invaluable in assigning bands to out-of-plane deformational vibrations (γ_{OH}) in 900-700 cm^{-1} region *(Fig. 11)*. For L-ascorbic acid it is observed seven bands but for the D-isoascorbic acid only four. The observation of seven bands in this range for one of the isomers is due to the overlap of the bands. Importantly, the isotope effect occurring in this spectral range is miraculous for this type of vibration in the IINS spectra. The number of bands attributed to the vibrations of the hydrogen bridge in the lower wavenumber range is respectively: eight (for isomer L) and four (for isomer D-iso) *(Fig. 11)*.

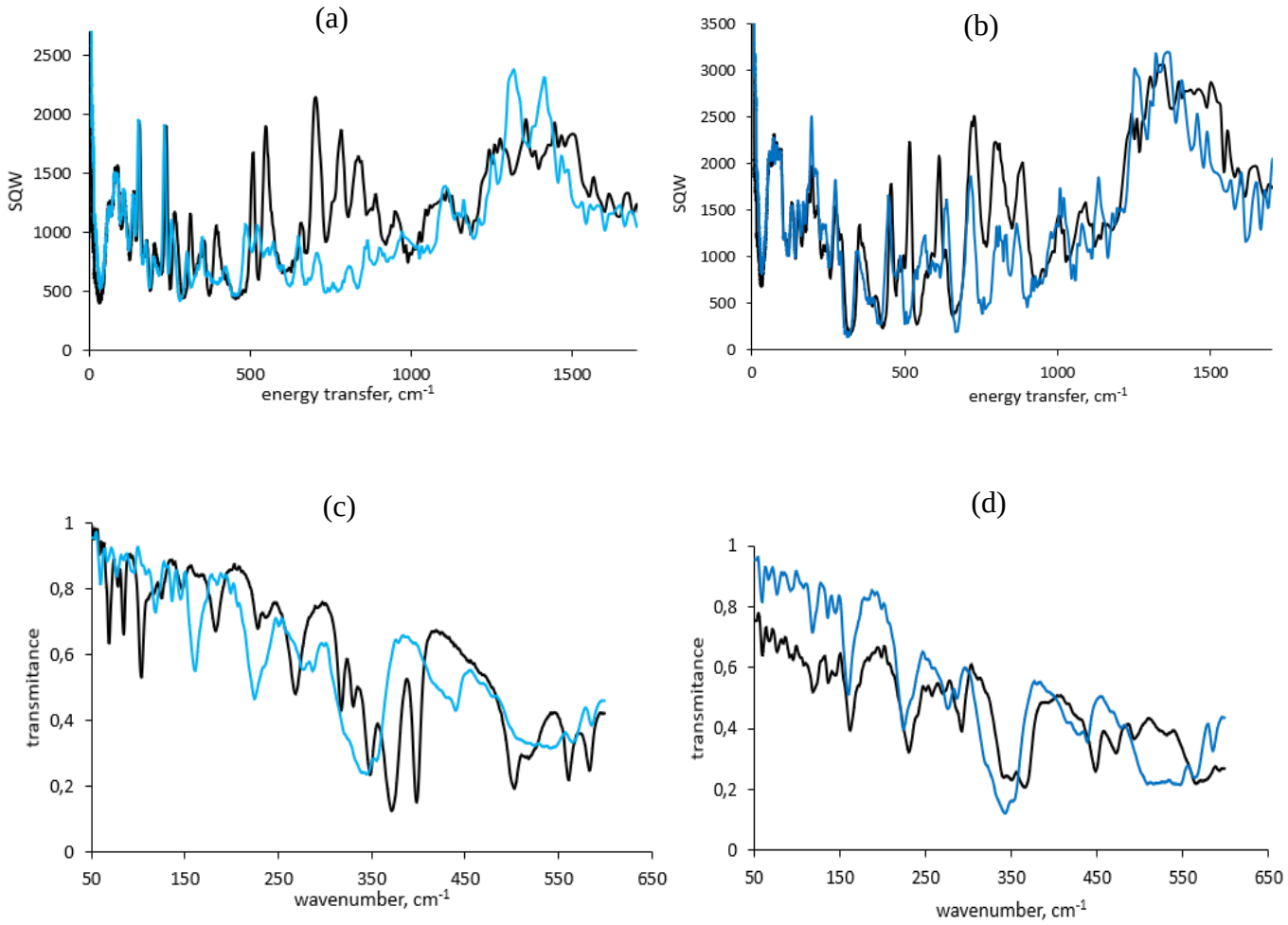

Figure 11. Normalized IINS in 0 – 1600 cm^{-1} region. (a-b) and FT-FIR in 50 – 600 cm^{-1} (c-d) spectra of (a, c) D-iso- and (b, d) L-ascorbic acids (black spectra) and its deuterated derivatives (blue spectra).

Overall, the number of bands assigned to the L isomer far exceeds the number of bands for the D isomer. Confirming this fact, a series of CPMD-solid simulations of the vibrational spectra of hydrogens calculations were made. The spectra obtained from the CPMD calculations was compared with the experimental spectrum in order to explain the number of bands coming from the vibrations of the stretching hydroxyl groups. Based on the results of the calculations, it is possible to more accurately assign bands to the appropriate vibrations of a part of a molecule. Thus, six bands are observed on the experimental L-ascorbic acid spectrum, of which: the band assigned to the vibration of the hydroxyl group marked on the structure ***3AA*** *(Fig. 9)* corresponds to the band number 8 *(Fig. 12);* ***2AA*** → (4); ***5AA, 6AA*** → (1, 2, 5, 6). However, the 6 bands correspond to the vibrations of the eight hydroxyl groups due to the presence of both L-ascorbic acid structures in the primitive cell *(Fig. 12).*

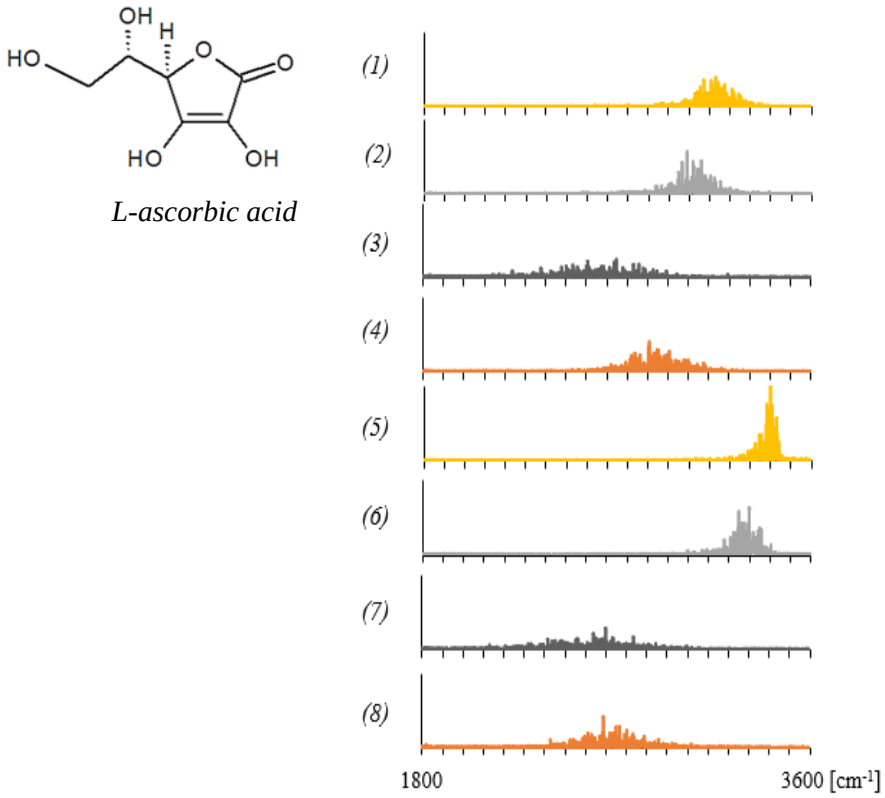

Figure 12. CPMD-solid simulations of the vibrational spectra of hydrogens calculations for L-ascorbic acid.

For the second isomer, only four signals are visible in the experimental spectra, the amount of which is consistent with the CPMD calculations *(Fig. 13).* This is due to the presence of one isomer in the primitive cell which is equivalent to the inability to form identical hydrogen bonds as the L isomer.

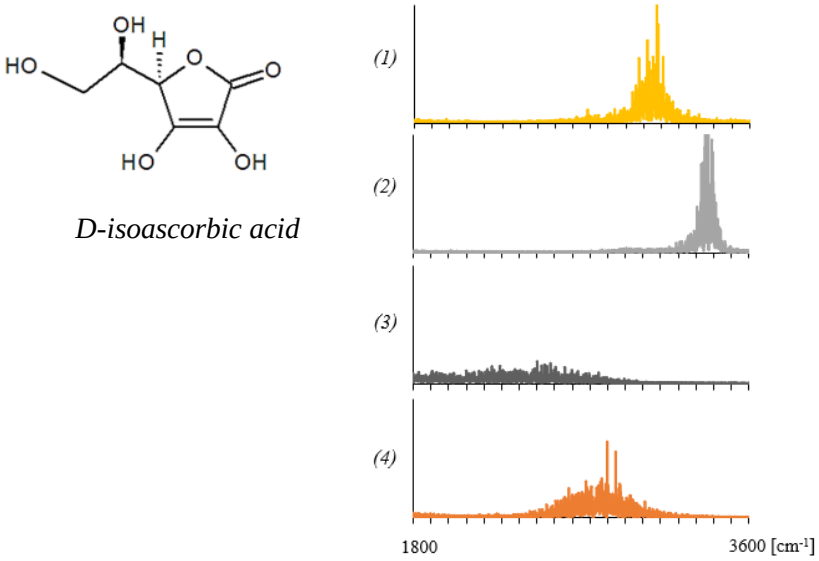

D-isoascorbic acid

Figure 13. CPMD-solid simulations of the vibrational spectra of hydrogens calculations for L-ascorbic acid.

DFT (Density Functional Theory) calculations were performed to test the possibility of proton transfer in intramolecular hydrogen bridge. For the monomers, calculations of proton transfer in the intramolecular hydrogen bridge and transfer of both protons were performed. The ΔE energy values were calculated based on the following formula:

$$\Delta E = 627{,}509\,(E_i - E_{min})$$

where,

E_i - energy of a given conformer,

E_{min} - the energy of the most stable conformer.

The distance between oxygen and hydrogen (O-H) was lengthened by 0.8 Å to 2.2 Å in increments of 0.1 Å. For both the transfer of one or two protons in the monomer, no two minima were observed on the potential energy curve. There is no possibility of proton transfer in the intramolecular hydrogen bridge. The results of the DFT calculations are very similar for both monomers: L-ascorbic acid and D-isoascorbic acid *(Fig. 14, 15).*

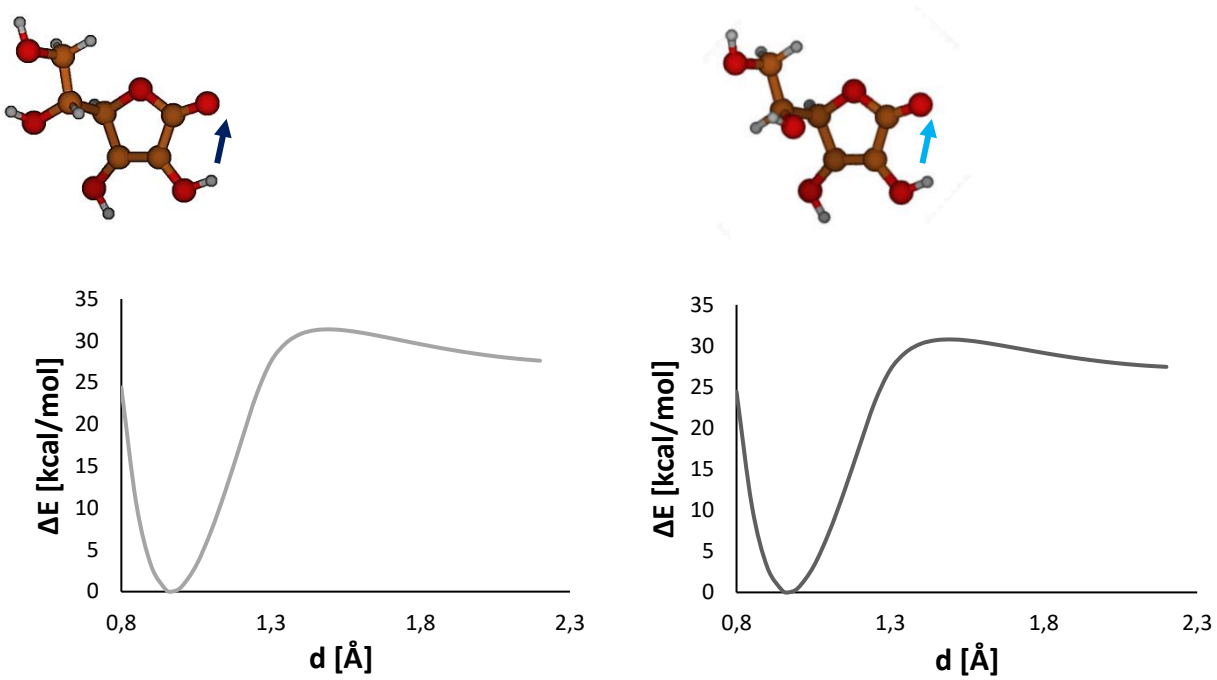

Figure 14. The potential energy profile for a gradual displacement of one proton within the intramolecular hydrogen bridge in L-ascorbic acid (left) and D-isoascorbic acid (right).

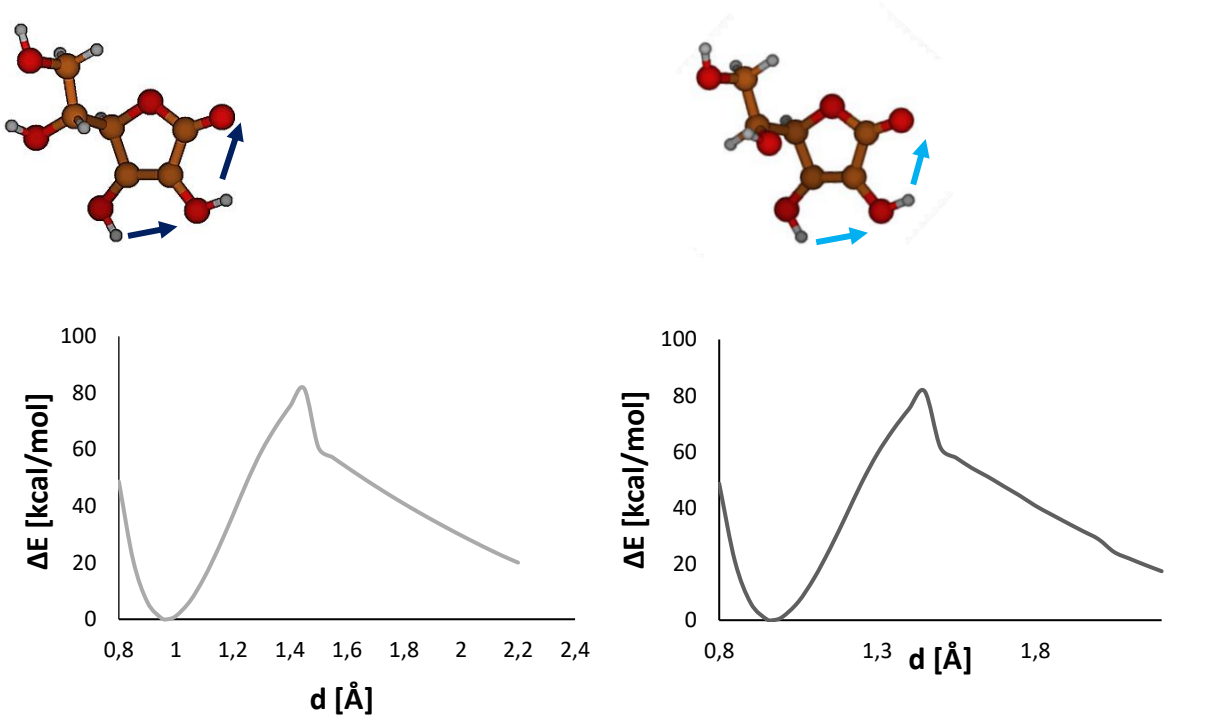

Figure 15. The potential energy profile for a gradual displacement of two protons within the intramolecular hydrogen bridges in L-ascorbic acid (left) and D-isoascorbic acid (right).

8. Summary

Participation in the *Summer Student Program* at the Joint Institute for Nuclear Research (JINR) in Frank Laboratory of Neutron Physics (FLNP) enabled me:

- learning about the properties and applications of the research molecules,
- better understanding of concepts such as isomer or isotope effect and using them in practice,
- understanding the operation of measuring equipment – NERA spectrometer,
- analysis and interpretation of vibrational spectra: IR, Raman and IINS,
- comparing the information that can be obtained about the studied molecule thanks to the combination of three spectroscopic methods,
- broadening the knowledge of non-covalent interactions like hydrogen bonding,
- understanding the importance of the formation of hydrogen bonds in the studied molecules and their influence on the interpretation of the spectra,
- taught me how to combine computational methods with experimental methods to get complete information about a system,
- broadened my knowledge and skills in DFT, PED and CPMD calculations.

Futhermore,

- learning about the structure and functioning of the Frank Laboratory of Neutron Physics and variety of researches performed at the Joint Institute for Nuclear Research,
- broadening the knowledge on the principles of operation of the IBR-2 reactor and other measuring equipment.

9. Acknowledgements

I would like to thank my supervisor Prof. Dr. Sc. A. Filarowski for the opportunity to participate in the internship, choosing the project topic, all help and support during the entire stay at the Institute.

I would also like to thank Dr. Sc. A. Jezierska, Dr. Sc. J. J. Panek for making a series of CPMD calculations. Thanks to this I was able to expand my knowledge about quantum mechanical methods.

I would also wish to thank Dr. E. V. Goremychkin for measuring the IINS spectra and for help with their interpretation.

10. References

1. D. B. McCormick, H. L. Greene (1994). *Vitamins*. In Burtis CA, Ashwood ER, editors: Tietz textbook of clinical chemistry, ed 2, Philadelphia, WB Saunders, 1275–1316.
2. A. K. Schlueter, C. S. Johnston (2011). *Vitamin C: Overview and Update.* Journal of Evidence-Based Complementary & Alternative Medicine, 16(1), 49–57.
3. V. Marisa, F. Carvalho, M. Lourdes, R. Albuquerque, M. Carvalho, F. Remio, (2012). *Adrenaline and Noradrenaline: Partners and Actors in the Same Play*. Neuroscience - Dealing with Frontiers, 1-5.
4. C. S. Johnston, F. M. Steinberg, R. B. Rucker (2013). *Ascorbic Acid*. Handbook of Vitamins, Fourth Edition, chapter 15.
5. A. Meneses, G. Liy-Salmeron, (2012). *Serotonin and emotion, learning and memory*. Reviews in the Neurosciences, 23(5-6), 1-3.
6. A. Hacişevkđ (2009). *An overview of ascorbic acid biochemistry*. Journal of Faculty of Pharmacy of Ankara University, 38(3), 233-255.
7. C. M. A. de Oliveira Lima (2020). *Information about the new coronavirus disease (COVID-19)*, Radiologia Brasileira, Mar/Abr, 53(2), 5-6.
8. J. Obi, S. M. Pastoresa, L. V. Ramanathan, J. Yanga, N. A. Halpern (2020). *Treating sepsis with vitamin C, thiamine, and hydrocortisone: Exploring the quest for the magic elixir*. Journal of Critical Care, 57, 231-239.
9. L. Zhang, Y. Liu, (2020). *Potential Interventions for Novel Coronavirus in China: A Systemic Review*. Journal of Medical Virology, 92, 479–490.
10. A. B. Nathens, M. J. Neff, G. J. Jurkovich, P. Klotz, K. Farver, J. T. Ruzinski (2002). *Randomized, prospective trial of antioxidant supplementation in critically ill surgical patients.* Annals of Surgery, 236(6), 814-822.
11. C. A. Rossetti, J. P. Real1, S. D. Palma (2020). *High Dose Of Ascorbic Acid Used In Sars Covid-19 Treatment: Scientific And Clinical Support For Its Therapeutic Implementation*. Ars Pharmaceutica, 61(2), 145-148.
12. S. Khan, S. Faisal, H. Jan (2020). *COVID-19: A brief overview on the role of Vitamins specifically Vitamin C as immune modulators and in prevention and treatment of SARS-Cov-2 infections*. Biomedical Journal of Scientific & Technical Research, 28(3), 21581-21584.
13. A. J. Ramirez-Cuesta, P. C. H. Mitchell (2013). *Neutrons and Neutron Spectroscopy.* Local Structural Characterisation, 173–224.

14. B. R. Holstein (2009). *Fundamental Neutron Physics: Introduction and Overview*. Journal of Physics G: Nuclear and Particle Physics, 36, 1-2.
15. E. Kartini (2007). *The Prospect of Neutron Scattering in the 21st Century: A powerful tool for materials research*. International Conference on Advances in Nuclear Science and Engineering in Conjunction with LKSTN, 317-324.
16. R. Pynn (1990). *Neutron scattering a primer*. LANSCE (Los Alamos Neutron Science Center).
17. Q. Berrod, K. Lagrené, J. Ollivier (2018). *Inelastic and quasi-elastic neutron scattering. Application to soft-matter.* EPJ Web of Conferences 188, JDN 23, 3-15.
18. R. Pynn (2009). *Introduction to Neutron Scattering, Chapter 2. Neutron Scattering—A Non-destructive Microscope for Seeing Inside Matter.* Neutron Applications in Earth, Energy and Environmental Sciences, Neutron Scattering Applications and Techniques, 1-25.
19. S. F. Parker (2006). *Inelastic Neutron Scattering Spectroscopy*. Handbook of Vibrational Spectroscopy, John Wiley & Sons, Ltd., 838-840.
20. P. C. H. Mitchell, S. F. Parker, A. J. Ramirez-Cuesta, J. Tomkinson (2005). *Vibrational Spectroscopy with Neutrons with Applications in Chemistry, Biology, Materials Science and Catalysis*. World Scientific, 1-150.
21. B. S. Hudson (2001). *Inelastic Neutron Scattering: A Tool in Molecular Vibrational Spectroscopy and a Test of ab Initio Methods.* The Journal of Physical Chemistry A, 105(16), 3949–3960.
22. G. Shirane, S. M. Shapiro, J. M. Tranquada (2004). *Neutron Scattering with a Triple-Axis Spectrometer. Basic Techniques.* Cambridge University Press, 16-35.
23. A. E. Pavlova, A. O. Petrova, P. I. Konik, K. A. Pavlov, S. V. Grigoriev (2021). *Inelastic Neutron Scattering Spectrometer INDIGO (Indirect Geometry) at the DARIA Compact Neutron Source.* Journal of surface investigation: X-ray, synchrotron and neutron techniques, 15(1), 70-74.
24. *https://nmi3.eu/neutron-research/techniques-for-/dynamics/time-of-flight spectroscopy.html*
25. F. Mezei, M. T. Caccamo, F. Migliardo, S. Magazù (2016). *Enhanced Performance Neutron Scattering Spectroscopy by Use of Correlation Techniques.*
26. I. Natkaniec, D. Chudoba, Ł. Hetmańczyk, V. Y. Kazimirov, J. Krawczyk, I. L. Sashin, (2014). *Parameters of the NERA spectrometer for cold and thermal moderators of the IBR-2 pulsed reactor.* Journal of Physics, Conference Series 554, 1-5.

27. A. V. Belushkin (1991). *IBR-2 – the fast pulsed reactor at Dubna.* Neutron News, 2(2), 14–18.
28. V. N. Shvetsov *(2017). Review Neutron Sources at the Frank Laboratory of Neutron Physics of the Joint Institute for Nuclear Research.* Quantum Beam Science, 1(6), 1-6.
29. M. Frontasyeva (2005). *Radioanalytical Investigations at the IBR-2 Reactor in Dubna.* Neutron News, 16 (3), 24-25.
30. *http://flnph.jinr.ru/en/facilities/ibr-2/instruments/nera*
31. R. S. Pinna, M. Zanetti, S. Rudi´c, S. F. Parker (2018). *The TOSCA Spectrometer at ISIS: the Guide Upgrade and Beyond.* IOP Conference Series: Journal of Physics, 1021, 1-4.
32. G. Škoro, G. Romanelli, S.Rudi´c, S. Lilley, F. Fernandez-Alonso (2020). *Discovery of new neutron-moderating materials at ISIS Neutron and Muon Source.* EPJ Web of Conferences 239, 17008, 1-4.
33. H. Cavendish, (1766). *Three Papers, Containing Experiments on Factitious Air, by the Hon. Henry Cavendish.* Philosophical Transactions of the Royal Society of London, 56(0), 141–184.
34. R. C. Olby (1966). *Chapter 3 - Antoine Lavoisier, 1743–1794. Late Eighteenth Century European Scientists*. Pergamon, 2, 67-93.
35. A. Keçebaş, M. Kayfeci (2019). *Hydrogen properties. Solar Hydrogen Production.* 3–29.
36. Z. A. Szydło (2020). *Hydrogen - some historical highlights*. Chemistry-Didactics-Ecology-Metrology, 25(1-2), 5-34.
37. G. F. Herzog (2021). *"isotope". Encyclopedia Britannica, Invalid Date, https://www.britannica.com/science/isotope. Accessed 16 August 2021*.
38. W. A. Van Hook (2011). *Isotope effects in chemistry*. Nukleonika, 56 (3), 217−240.
39. A. Kohen, H. Limbach (2006). *Isotope Effects in Chemistry and Biology*. CRC Press, Taylor & Francis Group, 1-1096.
40. L. Sobczyk, M. Obrzud, A. Filarowski (2013). *H/D Isotope Effects in Hydrogen Bonded Systems.* Molecules, 18 (4), 4467-4476.
41. N. Bonanos, A. Huijser, F. W. Poulsen (2015). *H/D isotope effects in high temperature proton conductors.* Solid State Ionics, 27, 9-13.
42. M. Tachikawa, M. Shiga (2005). *Geometrical H/D Isotope Effect on Hydrogen Bonds in Charged Water Clusters.* Journal of the American Chemical Society, 127 (34), 11908-11909.

43. R. Nakayama, M. Maesato (2021). *Heavy Hydrogen Doping into ZnO and the H/D Isotope Effect.* Journal of the American Chemical Society, 143 (17), 6616-6621.
44. M. Tachikawa, M. Shiga (2005). *Geometrical H/D Isotope Effect on Hydrogen Bonds in Charged Water Clusters.* Journal of the American Chemical Society, 127(34), 11908–11909.
45. M. J. Frisch, G. W. Trucks, H. B. Schlegel, G. E. Scuseria, M. A. Robb, J. R. Cheeseman, G. Scalmani, V. Barone, G. A. Petersson (2016). *Gaussian 16, Revision C.01; Gaussian, Inc., Wallingford, CT.*
46. J. M. L. Martin and C. Van Alsenoy (1995). *Gar2ped, University of Antwerp.*
47. W. Humphrey, A. Dalke and K. Schulten (1996). *Visual Molecular Dynamics.* The Journal of Molecular Graphics, 14, 33–38.
48. *Mercury—Crystal Structure Visualisation. Available at: http://www.ccdc.cam.ac.uk/Solutions/CSDSystem/Pages/Mercury.aspx*
49. T. Williams, C. Kelley (2010). *Gnuplot 4.4: an interactive plotting program. http://gnuplotsourceforge.net/*